AMERICAN ACADEMY OF OPHTHALMOLOGY®

Loss of Corneal Nerves and Corneal Haze in Patients with Fuchs' Endothelial Corneal Dystrophy with the Transcription Factor 4 Gene Trinucleotide Repeat Expansion

Matthew Gillings, MD,[1,] Andrew Mastro, MD,[1,*] Xunzhi Zhang,[2] Kelly Kiser, MD,[1] Jane Gu,[1] Chao Xing, PhD,[2,3,4] Danielle M. Robertson, OD, PhD,[1] W. Matthew Petroll, PhD,[1] V. Vinod Mootha, MD[1,2]*

Objective: Seventy percent of Fuchs' endothelial corneal dystrophy (FECD) cases are caused by an intronic trinucleotide repeat expansion in the transcription factor 4 gene (*TCF4*). The objective of this study was to characterize the corneal subbasal nerve plexus and corneal haze in patients with FECD with (RE+) and without the trinucleotide repeat expansion (RE−) and to assess the correlation of these parameters with disease severity.

Design: Cross-sectional, single-center study.

Participants: Fifty-two eyes of 29 subjects with a modified Krachmer grade of FECD severity from 1 to 6 were included in the study. Fifteen of the 29 subjects carried an expanded *TCF4* allele length of $\geq$ 40 cytosine-thymine-guanine repeats (RE+).

Main Outcomes Measures: In vivo confocal microscopy assessments of corneal nerve fiber length (CNFL), corneal nerve branch density, corneal nerve fiber density (CNFD), and anterior corneal stromal backscatter (haze); Scheimpflug tomography densitometry measurements of haze in anterior, central, and posterior corneal layers.

Results: Using confocal microscopy, we detected a negative correlation between FECD severity and both CNFL and CNFD in the eyes of RE+ subjects (Spearman $\rho = -0.45$, $P = 0.029$ and $\rho = -0.62$, $P = 0.0015$, respectively) but not in the eyes of RE− subjects. Additionally, CNFD negatively correlated with the repeat length of the expanded allele in the RE+ subjects (Spearman $\rho = -0.42$, $P = 0.038$). We found a positive correlation between anterior stromal backscatter and severity in both the RE+ and RE− groups ($\rho = 0.60$, $P = 0.0023$ and $\rho = 0.44$, $P = 0.024$, respectively). The anterior, central, and posterior Scheimpflug densitometry measurements also positively correlated with severity in both the RE+ and RE− groups ($P = 5.5 \times 10^{-5}$, 2.5×10^{-4}, and 2.9×10^{-4}, respectively, after adjusting for the expansion status in a pooled analysis. However, for patients with severe FECD (Krachmer grades 5 and 6), the posterior densitometry measurements were higher in the RE+ group than in the RE− group ($P < 0.05$).

Conclusions: Loss of corneal nerves in FECD supports the classification of the *TCF4* trinucleotide repeat expansion disorder as a neurodegenerative disease. Haze in the anterior, central, and posterior cornea correlate with severity, irrespective of the genotype. Quantitative assessments of corneal nerves and corneal haze may be useful to gauge and monitor FECD disease severity in RE+ patients. *Ophthalmology Science 2023;3:100214 © 2022 by the American Academy of Ophthalmology. This is an open access article under the CC BY-NC-ND license (http://creativecommons.org/licenses/by-nc-nd/4.0/).*

Supplemental material available at www.ophthalmologyscience.org.

Fuchs' endothelial corneal dystrophy (FECD) is a common age-related degenerative disorder affecting 4% of Whites in the United States and the leading indication for keratoplasty in the developed world.[1,2] Fuchs' endothelial corneal dystrophy is characterized by the progressive loss of the normal morphology and cell density of the corneal endothelium accompanied by diffuse thickening of its basement membrane (Descemet's membrane) with focal excrescences called guttae.[3] Patients experience symptoms of glare, diurnal fluctuation in vision, and loss of vision as a result of the guttae, endothelial cell loss, corneal edema, and scarring.[4]

Recently, the potential for treating FECD has been transformed by the discovery that an intronic trinucleotide repeat expansion in the transcription factor 4 gene (*TCF4*) accounts for 70% of FECD cases in the United States.[5–8] Expansions of $\geq$ 40 cytosine-thymine-guanine (CTG) repeats at this gene locus confer significant risk for the development of FECD.[6] Expanded cytosine-uracil-guanine (CUG) repeat RNA molecules accumulate in the nuclei of

https://doi.org/10.1016/j.xops.2022.100214
ISSN 2666-9145/22

corneal endothelial cells of subjects with the triplet repeat expansion.[9] These mutant repeat RNA species bind and functionally sequester the muscleblind-like family of splicing factors, resulting in the missplicing of their target exons.[10] We recently observed that the missplicing of muscleblind-like−sensitive genes and the aberrant expression of key extracellular matrix genes occur early in the disease course in the corneal endothelium of presymptomatic subjects with the repeat expansion and foreshadow the upregulation of molecular pathways related to fibrosis, mitochondrial dysfunction, and immune cell activation, pathogenic changes observed late in the FECD disease course.[11]

These observations open the possibility of preventing FECD disease onset or progression with molecular therapies early in the disease course before the onset of irreversible loss of endothelial cells, fibrosis, and corneal edema. We and others have proposed therapeutic strategies that target the *TCF4* trinucleotide repeat expansion, including the use of gene editing,[12] antisense oligonucleotides,[13−15] duplex RNAs,[16] trinucleotide repeat-targeting catalytically dead Cas9,[17] and small molecules that bind with repeat RNA.[18]

The slow rate of FECD disease progression and endothelial cell loss, however, poses challenges to clinical trial design and selection of outcome measures to assess the efficacy of potential molecular therapies over a reasonable duration. The validation of corneal imaging biomarkers that correlate with FECD severity in patients with the trinucleotide repeat expansion may facilitate clinical trials of precision medicines.

Although FECD is primarily a disease affecting the corneal endothelium, structural and morphologic changes occur in all pre-Descemet's corneal layers that are detectible by both in vivo confocal microscopy and Scheimpflug tomography. Studies on heterogenous FECD cohorts have revealed that the loss of the subbasal nerve plexus and stromal haze correlate with disease severity[19−23]; however, it is unknown whether these changes are applicable to patients with the *TCF4* repeat expansion. In this study, we aimed to quantify the changes in the subbasal nerve plexus and stroma using in vivo confocal microscopy and Scheimpflug tomography and to assess whether these changes correlate with disease severity in patients with FECD with the *TCF4* trinucleotide repeat expansion (RE+) and in patients without the expanded repeat (RE−).

Methods

Study Participants

This was a cross-sectional, single-center study. The study was conducted in compliance with the tenets of the Declaration of Helsinki and with the approval of the institutional review board of the University of Texas Southwestern Medical Center. All study subjects were recruited from the cornea referral practice at the University of Texas Southwestern. After informed consent, the subjects underwent a complete eye examination including slit lamp biomicroscopy by a cornea fellowship-trained ophthalmologist (V.V.M.) to assess the corneal endothelium using the modified Krachmer FECD grading scale: grade 0: no central guttae; grade 1: up to 12 scattered central guttae; grade 2: ≥ 12 scattered central guttae; grade 3: 1- to 2-mm confluent central guttae; grade 4: 2 to 5 mm of confluent central guttae; grade 5: > 5-mm confluent central guttae without stromal edema; grade 6: > 5-mm confluent central guttae with stromal edema.[24] Genomic DNA from peripheral blood of subjects was used to genotype the *TCF4* CTG18.1 triplet repeat polymorphism using a combination of short tandem repeat and triplet repeat primed polymerase chain reaction assays, as we have previously described.[6,7] An allele length of ≥ 40 CTG repeats was considered an expanded allele as in previous studies.[6,7]

Fifty-two eyes with FECD Krachmer grades 1 to 6 from 15 individuals with the repeat expansion and 14 individuals without the repeat expansion were selected from our University of Texas Southwestern Medical Center FECD cohort for this imaging substudy conducted from July 2018 to December 2020. On the study visit for corneal imaging, the subjects were re-examined by the same investigator (V.V.M.) using slit lamp biomicroscopy to document the current Krachmer grade disease severity of their eyes. The eyes of subjects who had previously undergone keratoplasty or had a history of prior herpes simplex or zoster keratitis were excluded. Eyes of subjects with diabetes mellitus, contact lens use without corneal fluorescein staining, or mild dry eye (≤ grade 1 Dry Eye WorkShop [DEWS] dry eye severity grading scheme[25]) at the time of imaging were not excluded. Available medical records of subjects with diabetes were reviewed for details of treatment and glycemic control.

Corneal Imaging

Fifty-two eyes of 29 patients underwent Scheimpflug Pentacam imaging (OCULUS), of which 49 eyes of 27 patients also underwent in vivo confocal microscopy through-focusing (CMTF) using the Heidelberg Retina Tomograph with Rostock Cornea Module (Heidelberg Engineering, GmBH) that was modified for remote-controlled scanning and real-time image streaming.[26−28] The investigators performing the imaging data acquisition and analyses (M.G., A.M., K.K., J.G., M.P., D.R.) were masked to the Krachmer grade severity of disease and genotype of the study subjects. One group of investigators (A.M., J.G.) independently analyzed the Scheimpflug imaging data and were masked to the CMTF data analysis performed by the second group of investigators (M.G., K.K.).

Scheimpflug tomography in all subjects was performed in standardized low ambient light conditions in a room without windows located in the ophthalmic imaging suite of the Aston Ambulatory Care Center eye clinic at the University of Texas Southwestern Medical Center. For Scheimpflug imaging, the "densitometry" display of each eye was derived by the instrument's software (Pentacam version 1.22r05) and exported as a high-resolution image. The "densitometry" images provided by the Pentacam software were evaluated for the quantitative measure of corneal backscatter (haze). Densitometry values are expressed in grayscale units and range from 0 (completely clear) to 100 (completely opaque). The densitometry data are broken down by the software into an anterior 120-μm layer (epithelium, subbasal nerve plexus, and anterior stroma), central layer (midstroma), and posterior 60-μm layer (posterior stroma, Descemet's membrane, and endothelium). Densitometry data are further broken down into concentric rings composed of a central 0 to 2 mm, 2 to 6-mm, 6 to 10-mm, and 10 to 12-mm optical zones. In this study, we analyzed only the central 0 to 6-mm optical zone because this is the most applicable to visual function. To calculate densitometry values for the central 0 to 6 mm optical zone, the 0 to 2-mm and 2 to 6-mm zones were combined using the methods previously described by Hirabayashi et al.[29]

Confocal microscopy through-focusing imaging was performed as previously described.[28] Briefly, before CMTF, eyes were anesthetized with 1 drop of proparacaine. An ophthalmic lubricant gel (Systane gel, Alcon) was used to optically couple the Tomocap to the objective and to applanate the cornea. Several continuous CMTF scans were obtained from the endothelium to epithelium to maintain contact with the cornea during the scan. Images were collected from the central region of the cornea using the Heidelberg Retina Tomograph streaming software function, with the acquisition rate set to 30 frames per second, a lens speed of 60 μm/second, and a step size between images of approximately 2 μm. The field of view for each 384 × 384 pixel image was 400 × 400 μm. Confocal microscopy through-focusing scans were obtained with the gain manually set to 20. The same Heidelberg Retina Tomograph with Rostock Cornea Module confocal microscope was used to obtain images of the subbasal nerve plexus. For these nerve scans, the autogain feature was enabled and image depth was manually controlled to focus on the subbasal nerve plexus, collecting sequences of images of multiple distinct regions of the cornea.

Confocal microscopy through-focusing analysis was performed using a custom software as previously reported.[28,30] The area under the image intensity versus depth curve for the first 50 μm of the anterior stroma was calculated using a baseline set at a pixel intensity of 15. The beginning of the anterior stroma was identified as the interface between the subbasal nerve plexus and underlying stroma. Anterior stromal backscatter (haze) was expressed in arbitrary confocal backscatter units, which are defined as μm × pixel intensity. Confocal microscopy through-focusing analysis was completed by a single observer (M.G.) who was masked to the subject's Krachmer grade and genotype. Confocal microscopy through-focusing curves with evidence of excessive movement or those that lacked clear subbasal nerve plexus and anterior stromal peaks were excluded.

The nerve image scans were analyzed using MetaMorph. Images with nerves in focus across the entire image were selected for analysis, and if necessary, multiple images were aligned to keep the neve plexus in focus across the entire image.[31] As previously reported, 8 unique images that had less than approximately 20% overlap were used for analysis to approximate the value of the entire subbasal nerve plexus.[32] The nerves were traced using the MetaMorph multiline-tracing tool, and the total nerve length was calculated and reported in arbitrary units per frame as the corneal nerve fiber length (CNFL). The number of individual nerves excluding branches per image was recorded as the corneal nerve fiber density (CNFD). Branches were defined as nerve fibers less than approximately 50% of the longer continuous nerve segment. The total number of branch points per image was recorded as the corneal nerve branching density (CNBD). The subbasal nerve plexus imaging analysis was performed by 2 observers (K.K., M.G.) who were masked to the Krachmer grade and genotype.

Statistical Analysis

Demographic and clinical information was summarized as counts and percentage; age was summarized as median. Scheimpflug imaging measurements were summarized as median and interquartile range. Comparisons of the demographic and clinical phenotypic features between the RE+ and RE− groups were performed using a 2-sample *t* test for age and Fisher exact test for binary traits. Comparisons of confocal and Scheimpflug imaging parameters between eyes of the same severity in the RE+ and RE− groups were made using the Wilcoxon−Mann−Whitney test. Spearman rank correlations between the imaging measurements and the Krachmer grade were calculated and tested in the 2 groups, separately. In the RE+ group, Spearman rank correlations between the imaging measurements and repeat lengths of the expanded allele were also calculated and tested. We also used multiple linear regression models adjusting for the expansion status to examine the correlations. Software R (version 4.0.0) was used for statistical analysis. A P value of < 0.05 was considered statistically significant.

Results

Demographic Characteristics of Study Subjects

Study participant demographic characteristics and pertinent past medical history are summarized in Table 1. There is an approximately 2:1 female to male ratio in both the RE+ and RE− groups, which is consistent with the natural female predisposition for FECD.[33] Details of the management and glycemic control in the study subjects with diabetes mellitus are summarized in Table S1 (available at www.ophthalmologyscience.org). The Krachmer grades and trinucleotide repeat expansion status of the eyes in the entire cohort are shown in Table 2. A list of the repeat lengths for the RE+ group is shown in Table S2 (available at www.ophthalmologyscience.org).

In Vivo Confocal Microscopy

Analysis of the in vivo subbasal nerve plexus images revealed statistically significant negative correlations of CNFL and CNFD with the Krachmer grade in the RE+ eyes ($\rho = -0.45$, $P = 0.029$ and $\rho = -0.62$, $P = 0.0015$, respectively) but not in the RE− eyes (Fig 1A−C; Table 3). There was no statistically significant correlation between CNBD and the Krachmer grade in either RE+ or RE− group, but a multiple linear regression model adjusting for the expansion status (RE+ or RE−) did show a significant negative correlation in the entire cohort ($P = 0.026$; Fig 1D; Table 3). The CNFL and CNFD values were significantly lower in the RE+ eyes with severe FECD

Table 1. Baseline Participant and Ocular Characteristics.

	No. (%) of Participants	
	With Repeat Expansion (N = 15)	*Without Repeat Expansion (N = 14)*
Sex		
Male	4 (27)	4 (29)
Female	11 (73)	10 (71)
Age, median, yrs	66	62
Race/ethnicity		
Non-Hispanic White	15 (100)	9 (64)
Non-Hispanic Black/ African American	0 (0)	4 (29)
Asian/Indian	0 (0)	1 (7)
Diabetes mellitus*	3 (20)	5 (35)
Contact lens use	1 (7)	1 (7)
Dry eye disease	3 (20)	6 (42)

With the exception of race/ethnicity ($P = 0.02$), no differences were found to be significant between the 2 populations. Fisher exact tests were used for all characteristics except for age where a 2-tailed t test was used.
*Details of management and control of diabetes mellitus are summarized in Table S1 (available at www.ophthalmologyscience.org/).

Table 2. Summary of Eyes by Krachmer Grade and Expansion Status

Krachmer Grade*	Entire Cohort (N = 52)	RE+ (n = 26)	RE− (n = 26)
1	4	1	3
2	12	6	6
3	6	1	5
4	11	7	4
5	8	4	4
6	11	7	4

*Krachmer grade of Fuchs' endothelial corneal dystrophy for the 52 eyes of 29 patients. RE+ = repeat expansion positive (RE+); RE− = repeat expansion negative.

(Krachmer grade 5 or 6) compared with the RE− eyes with severe FECD ($P < 0.05$; Table 3).

In the CMTF scans, the anterior stromal backscatter (haze) was visualized and quantified in the form of a peak immediately after the peak normally associated with the subbasal nerve plexus (Fig 2A, B). For quantification of anterior stromal haze, a consistent 50 µm slice of the anterior corneal stroma underlying the subbasal nerve plexus that includes this anterior stromal haze peak was imaged (Fig 2B). There was a positive correlation between anterior stromal haze and the Krachmer grade in both the RE+ and RE− groups ($\rho = 0.60$, $P = 0.0023$ and $\rho = 0.44$, $P = 0.024$, respectively; Fig 2C; Table 3).

Scheimpflug Tomography

The anterior (120-µm layer of the cornea), central, and posterior (60-µm layer) densitometry measurements were all positively correlated with the Krachmer grade in both the RE+ and RE− eyes ($P = 5.5 \times 10^{-5}$, 2.5×10^{-4}, and 2.9×10^{-4}, respectively, adjusting for the expansion status; Fig 3; Table 3). For patients with severe FECD (Krachmer grades 5 and 6), the posterior densitometry measurements were higher in the RE+ group than in the RE− group ($P < 0.05$) ($P < 0.05$; Table 3).

Correlation of Imaging Parameters to Repeat Length

Correlations of confocal imaging parameters (CNFL, CNBD, CNFD, and anterior corneal stromal backscatter) and Scheimpflug tomography densitometry measurements to repeat length of the expanded allele in the RE+ group are shown in Figures S1 to S7 (available at

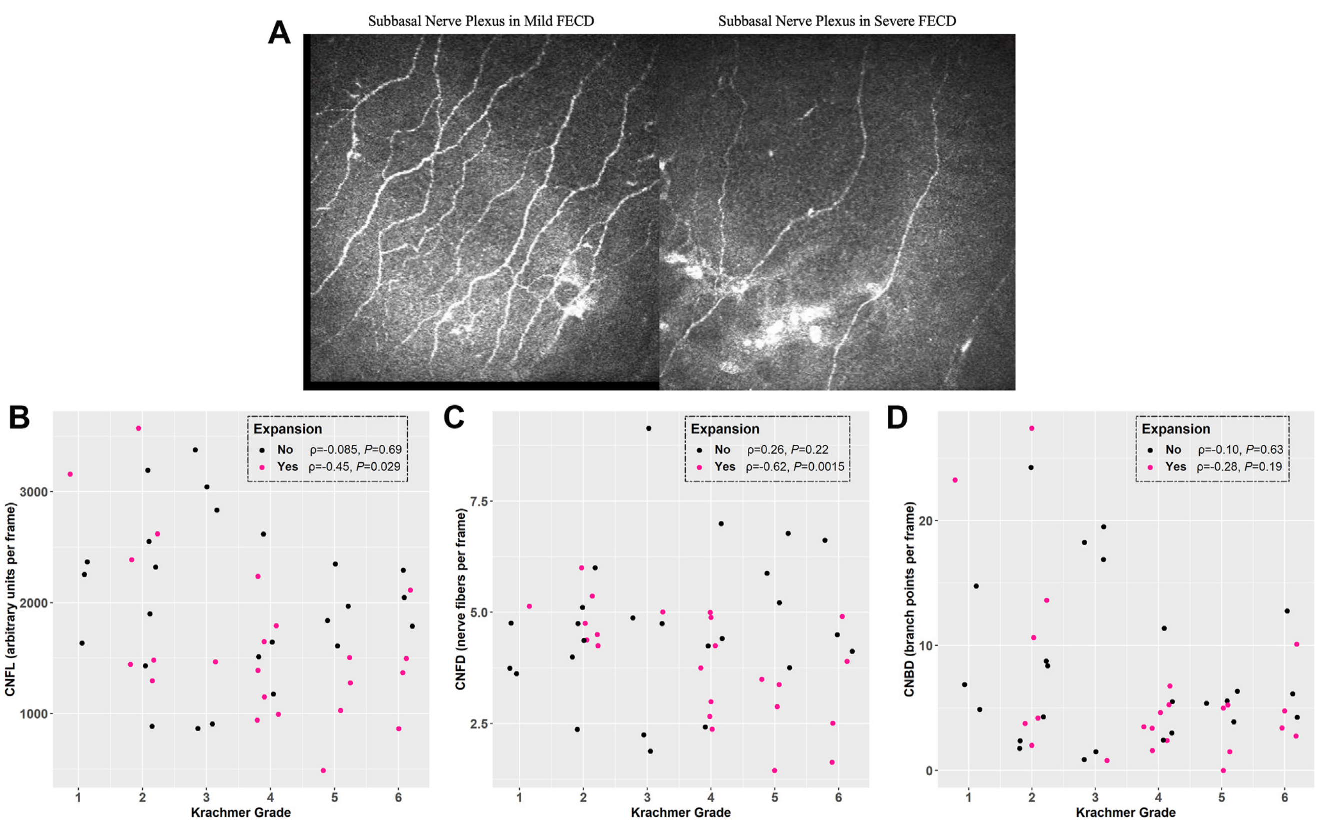

Figure 1. Subbasal nerve plexus in Fuchs' endothelial corneal dystrophy (FECD). **A**, Representative confocal microscopy through-focusing (CMTF) image of subbasal nerve plexus from eye with mild FECD (Krachmer grade = 2) of repeat expansion positive (RE+) patient (left panel) compared with eye with severe FECD (Krachmer grade = 5) of RE+ patient (right panel). **B**, Corneal nerve fiber length (CNFL) versus FECD severity. **C**, Corneal nerve fiber density (CNFD) versus FECD severity. **D**, Corneal nerve branch density (CNBD) versus FECD severity. Spearman correlation between CMTF subbasal nerve plexus imaging parameters of CNFL, CNFD, and CNBD and modified Krachmer grade of FECD disease severity from 1 to 6.

Table 3. Confocal and Scheimpflug Imaging Parameters Stratified by FECD Severity Measured by the Krachmer Grade

	Eyes with FECD without the Repeat Expansion			Eyes with FECD with Repeat Expansion			
	Mild (9 Eyes)	*Moderate (9 Eyes)*	*Severe (8 Eyes)*[†]	*Mild (7 Eyes)*	*Moderate (8 Eyes)*	*Severe (11 Eyes)*[‡]	**P Value** [§]
Confocal nerve fiber length*	2252.37 (731.33)	1643.56 (1659.38)	1968.68 (355.55)	2385.63 (1426.35)	1428.49 (572.87)	1323.30 (511.72)[‖]	0.036
Confocal nerve fiber density	4.38 (1.00)	4.40 (2.45)	5.22 (1.94)	4.75 (0.81)	4.00 (1.99)	3.13 (1.32)[‖]	0.45
Confocal nerve branching density	6.88 (4.45)	5.50 (14.45)	5.56 (1.42)	10.63 (14.47)	3.44 (2.60)	4.08 (2.63)	0.026
Confocal anterior stroma 50 μm backscatter (CBU)	3152.50 (573.80)	3524.90 (744.60)	3697.25 (1450.50)	3326.20 (522.45)	3782.10 (780.40)	5154.03 (3151.50)	0.00065
Scheimpflug anterior 120 μm backscatter (GSU)	19.87 (7.35)	23.17 (2.85)	23.39 (8.21)	23.01(1.68)	22.18 (0.63)	27.99 (5.08)	$5.48e^{-05}$
Scheimpflug mid cornea (GSU)	16.61 (1.89)	17.01 (1.90)	17.20 (3.31)	16.07 (0.77)	15.62 (0.55)[‖]	18.61 (2.09)	0.00025
Scheimpflug posterior 60 μm (GSU)	11.29 (3.01)	12.05 (2.42)	12.74 (0.62)	12.80 (1.35)	12.59 (1.42)	14.96 (1.49)[‖]	0.00029

CBU = confocal backscatter units; FECD = Fuchs' endothelial corneal dystrophy; GSU = grayscale units.
Median and interquartile range are presented. Mild: Krachmer grade = 1 or 2; moderate: Krachmer grade = 3 or 4; severe Krachmer grade = 5 or 6.
*Corneal nerve fiber length units are arbitrary units given by the tracing software in MetaMorph.
†Subbasal nerve plexus parameters were unable to be assessed for one of these eyes.
‡Three of these eyes did not undergo confocal imaging.
§Association between the parameter and Krachmer grade by fitting a linear regression model adjusting for the expansion status.
‖Significant difference between eyes of the same severity in RE+ and RE− groups ($P < 0.05$) by the Wilcoxon−Mann−Whitney test.

www.ophthalmologyscience.org). Corneal nerve fiber density negatively correlated with the repeat length of the expanded allele in the RE+ subjects (Spearman $\rho = -0.42$, $P = 0.038$) (Fig S3). We found no statistically significant correlations between the 6 other imaging parameters and repeat length.

Discussion

Nucleotide repeat expansions are associated with > 50 human diseases, and they primarily exhibit a neurodegenerative phenotype.[34] Like peripheral neurons, corneal endothelial cells are derived from neural crest tissue, express neuronal markers, and are postmitotic after birth.[35] Our observation that loss of the subbasal nerve plexus correlates with disease severity in patients with FECD further supports the classification of the *TCF4* trinucleotide repeat disorder as a neurodegenerative disease. Although we also observed loss of CNFL and density loss in patients with FECD without the expansion, their correlations with disease severity did not reach statistical significance. In other neurodegenerative disorders mediated by DNA repeat expansions, such as myotonic dystrophy, alleles with longer repeat length correlate with increased disease severity and earlier onset.[36−38] Here, we found that the CNFD negatively correlated to the repeat length of the expanded allele in patients with FECD with the expansion.

The loss of corneal nerves occurs early in the disease course, well before the onset of corneal edema in subjects with FECD with the expanded repeat. The mechanism by which the attenuation of the subbasal corneal nerves occurs in FECD is not known but may result from loss of corneal endothelium triggered by the mutant repeat RNA.[11] Corneal endothelial cells are known to produce neuropeptides, including vasoactive intestinal peptides that maintain endothelium in their differentiated state and prevent cellular apoptosis; these neuropeptides may also be relevant to corneal nerve homeostasis.[19,39,40] Additionally, corneal endothelial cells express VEGF and nerve growth factor vital to maintenance of axons and neuronal growth.[41] However, the attenuation of subbasal nerve plexus observed in diabetes and herpes simplex keratitis may result in loss of the normal morphology and density of endothelial cells.[19] These findings support an alternate hypothesis that the primary loss of corneal nerves and decreased levels of neuropeptides contributes to endothelial disease pathogenesis in FECD.[19]

A limitation of our study was the inclusion of patients with diabetes mellitus or mild dry eye, which may have also contributed to the loss of corneal nerves.[42,43] However, the prevalence of these common, age-related comorbid conditions was comparable in the RE+ and RE− groups.

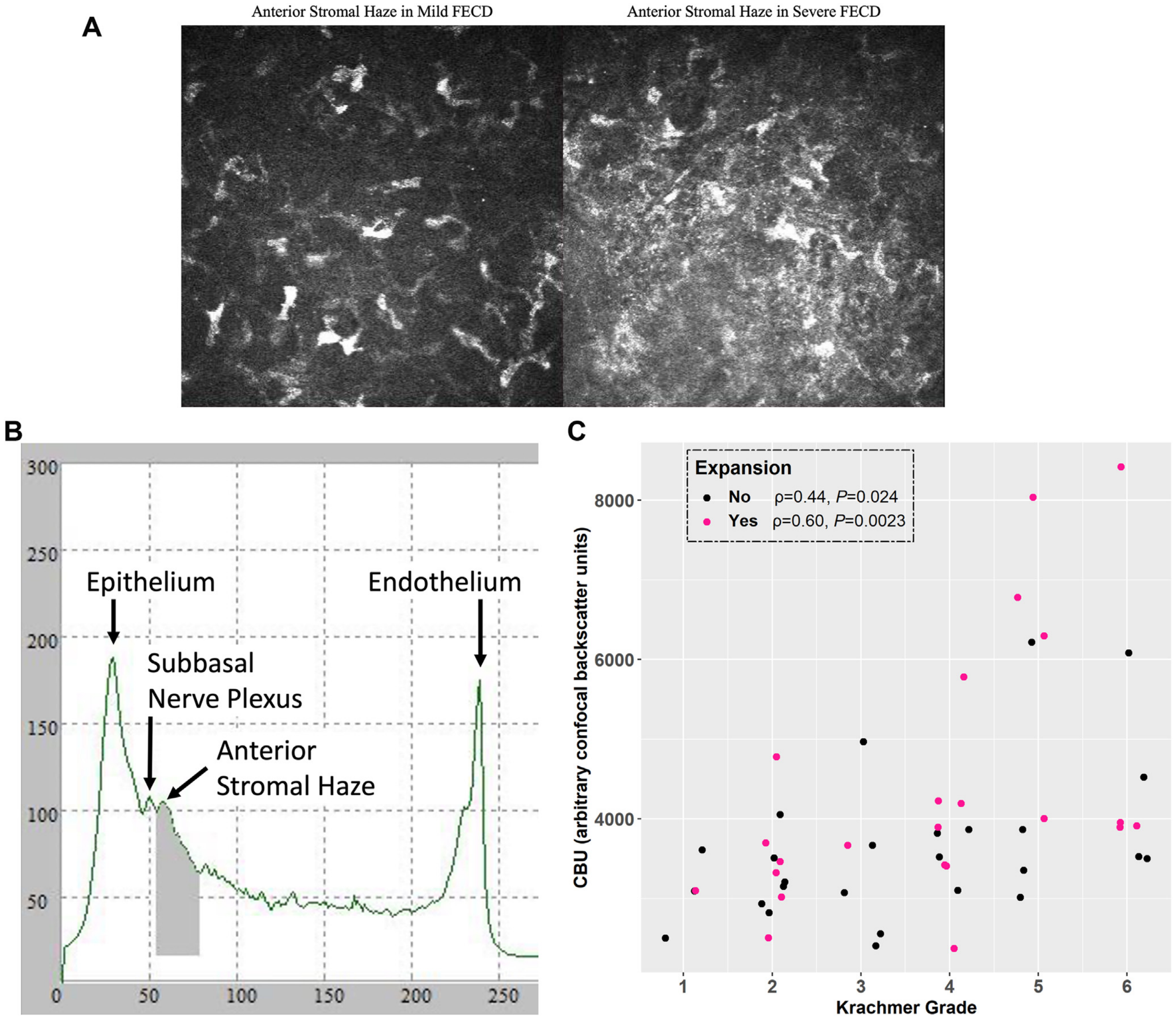

Figure 2. Corneal backscatter (haze) of the anterior stroma in Fuchs' endothelial corneal dystrophy (FECD). **A**, Representative confocal microscopy through-focusing (CMTF) image of keratocytes and reflectivity in the anterior stroma of eye with mild FECD (Krachmer grade = 2) of repeat expansion positive (RE+) patient compared with eye with severe FECD (Krachmer grade = 5) of RE+ patient. **B**, CMTF scan showing peaks corresponding to subbasal nerve plexus and anterior stroma haze in a subject with FECD. Anterior stromal haze was defined as the area under the CMTF curve of the first 50 μm of stroma underlying the subbasal nerve plexus and is reported in arbitrary confocal backscatter units (CBU). **C**, Anterior stromal haze (CBU) versus FECD disease severity from 1 to 6. Spearman correlation between CBU and modified Krachmer grade of FECD disease severity from 1 to 6.

Unlike the loss of the subbasal nerve plexus, which is particularly striking in patients with the *TCF4* triplet repeat expansion, corneal backscatter or haze in the various layers of the cornea does not seem to be specific to patients with FECD with the expansion. Using confocal microscopy, we were able to measure the backscatter in the 50 μm of stroma underlying the subbasal nerves in CMTF scans of the central cornea and establish that the previously observed correlation between anterior stromal backscatter and disease severity[22] applies to both RE+ and RE− patients with FECD. It is currently unknown why anterior corneal haze in the form of keratocyte activation develops early in the FECD course before the onset of clinically detectable edema. Anterior corneal haze increases further in late FECD, which has been attributed to corneal edema.[44] Interestingly, the anterior stromal haze improves only partially after successful endothelial keratoplasty and resolution of corneal edema.[28,45−47] These observations suggest that anterior stromal haze represents irreversible damage.

We found positive correlations between Scheimpflug densitometry measurements of the anterior 120-μm, central, and posterior 60-μm corneal layers and FECD severity in our entire cohort as has been previously reported in a

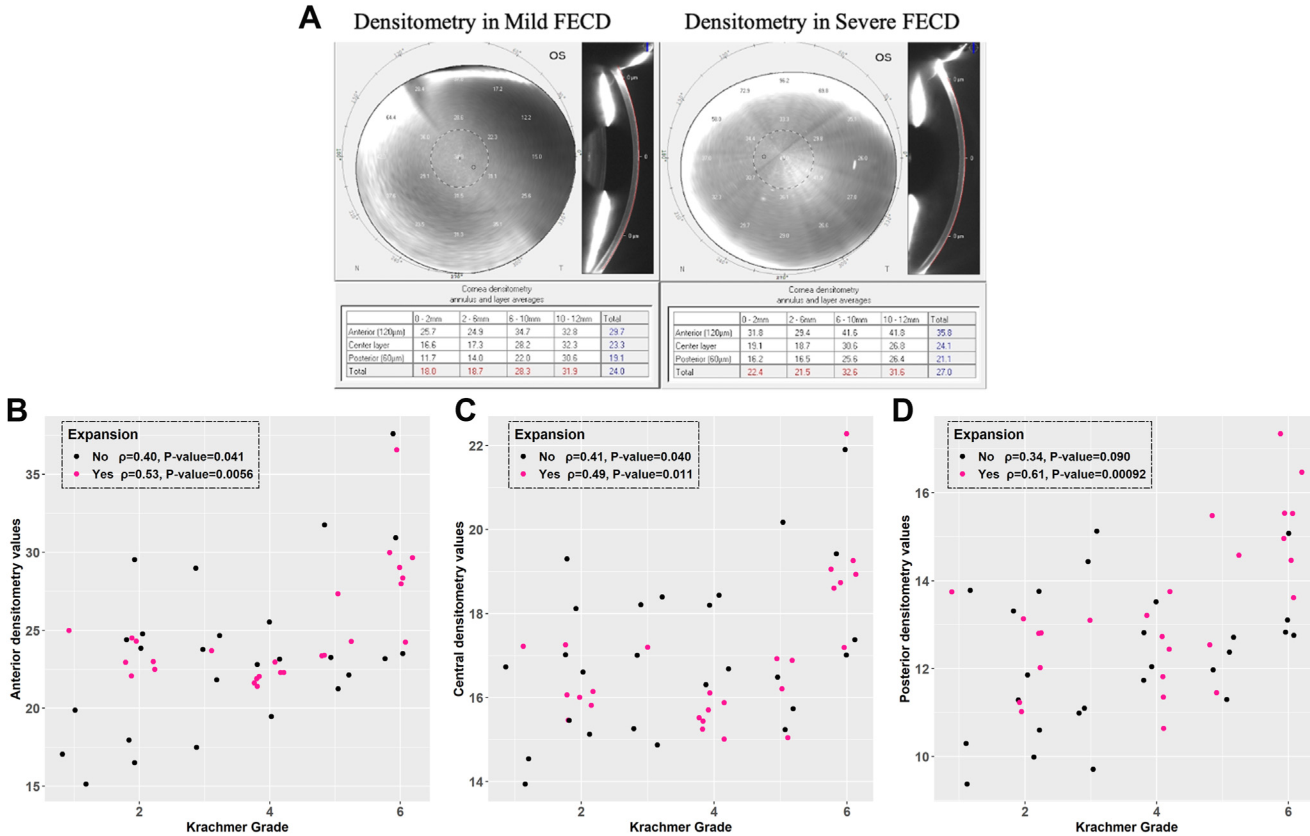

Figure 3. Corneal densitometry (backscatter or haze) of the anterior, middle, and posterior corneal layers. **A**, Representative Scheimpflug densitometry measurements of eye with mild Fuchs' endothelial corneal dystrophy (FECD) (Krachmer grade 1) of repeat expansion positive (RE+) patient (left panel) compared with eye with severe FECD (Krachmer grade 6) of RE+ patient. **B**, Densitometry of anterior 120-µm corneal layer versus FECD disease severity from 1 to 6. **C**, Densitometry of the central corneal layer versus FECD disease severity from 1 to 6. **D**, Densitometry of posterior 60-µm corneal layer versus FECD disease severity from 1 to 6. Spearman correlation between densitometry of anterior, central, and posterior corneal layers and modified Krachmer grade of FECD disease severity from 1 to 6.

heterogenous group of patients.[23] We found these correlations in both RE+ and RE− patients. Interestingly, Scheimpflug densitometry of the anterior 120-µm corneal layer has been shown to strongly correlate to the endothelial pump function in subjects with FECD assessed by measurements of the rate of recovery of cornea edema from contact lens−induced hypoxia.[48]

Increased densitometry of the posterior 60-µmlayer of the cornea in FECD may be explained by the higher posterior keratocyte density in the pre-Descemet's stromal layers,[19] fibrosis, edema, and the thickening of Descemet's membrane and guttae observed in FECD. A recent study reported that subjects with FECD with higher posterior corneal densitometry measurements had more visual disability.[49] Our finding in this study of higher posterior corneal densitometry in eyes with severe FECD in RE+ patients compared with eyes with severe FECD in RE− patients may help account for our previous observations that RE+ patients with FECD are at a higher risk of disease progression and need for keratoplasty than their RE− FECD counterparts.[8,50]

The slow rate of endothelial cell loss may limit the utility of endothelial cell density as an end point to assess the efficacy of a potential molecular therapy in a clinical trial setting. Additionally, measuring corneal endothelial cell morphology and density may be challenging and inaccurate in FECD using specular microscopy. The guttae obscure the visualization of overlying endothelial cells.[51] Additionally, the variation in the regional distribution and confluence of guttae can contribute to markedly different endothelial cell densities of the same patient's cornea.[51] Confocal microscopy may be an alternative to specular microscopy to evaluate regional differences of endothelial cell density in guttae and nonguttae areas of corneas of patients with severe FECD.[52] Scheimpflug tomography can generate useful pachymetry and posterior elevation maps, providing functional assessments of the health of the corneal endothelium in FECD.[53] However, because these Scheimpflug imaging parameters related to the thickness of the cornea are disturbed only in late FECD after significant loss of the endothelium and the onset of edema, they may not be ideal as end points to test the efficacy of molecular therapies intended to slow progression in patients with mild or moderate disease.

The morphological and structural changes in the pre-Descemet's layers of the cornea that occur early in the

FECD disease course and correlate with severity are pertinent to understanding the natural history of the disorder and therapeutic development. Quantitative assessments of corneal nerves and corneal haze may be useful outcome measures for therapeutic trials intended to slow or halt disease pathogenesis before the onset of significant and irreversible corneal haze and endothelial cell loss. However, longitudinal studies are certainly warranted to understand the natural history of disease progression of these imaging parameters in patients with FECD with the trinucleotide repeat expansion.

Acknowledgments

The authors thank the patients for their participation in this study. The authors thank David R. Corey, PhD, and Thomas Hohman, PhD, for helpful discussions on the project and manuscript. The authors acknowledge Perla Urbina and Daphne Fuerte for their efforts as research study coordinators for this project.

Footnotes and Disclosures

Originally received: March 26, 2022.
Final revision: July 30, 2022.
Accepted: August 19, 2022.
Available online: August 27, 2022. Manuscript no. XOPS-D-22-00054R1.

[1] Department of Ophthalmology, University of Texas Southwestern Medical Center, Dallas, Texas.

[2] Eugene McDermott Center for Human Growth and Development, University of Texas Southwestern Medical Center, Dallas, Texas.

[3] Department of Bioinformatics, University of Texas Southwestern Medical Center, Dallas, Texas.

[4] Department of Population and Data Sciences, University of Texas Southwestern Medical Center, Dallas, Texas.

Presented in part at the 2020 Association for Research in Vision and Ophthalmology Meeting, May 6, 2020 (Virtual).

*M.G. and A.M. contributed equally to this work.

Disclosures:

All authors have completed and submitted the ICMJE disclosures form.

The author(s) have no proprietary or commercial interest in any materials discussed in this article.

Supported by the National Institutes of Health, Bethesda, Maryland (grants R01EY022161 [V.V.M.] and P30EY030413 [V.V.M., W.M.P., D.R.]); from an unrestricted grant from Research to Prevent Blindness, New York (V.V.M.); and Harrington Scholar-Innovator Award from Harrington Discovery Institute (V.V.M.).

HUMAN SUBJECTS: Human subjects were included in this study. The study was conducted in compliance with the tenets of the Declaration of Helsinki and with the approval of the institutional review board of the University of Texas Southwestern Medical Center. All study subjects were recruited from the cornea referral practice at the University of Texas Southwestern. After informed consent, the subjects underwent a complete eye examination.

No animal subjects were used in this study.

Author Contributions:

Conception and design: Mootha.

Data collection: Gillings, Mastro, Kiser, Gu, Robertson, Petroll, Mootha.

Analysis and interpretation: Gillings, Mastro, Zhang, Xing, Petroll, Mootha.

Obtained funding: Mootha.

Overall responsibility: Gillings, Mastro, Xing, Petroll, Mootha.

Abbreviations and Acronyms:
CMTF = confocal microscopy through-focusing; **CNBD** = corneal nerve branch density; **CNFD** = corneal nerve fiber density; **CNFL** = corneal nerve fiber length; **FECD** = Fuchs' endothelial corneal dystrophy; **RE+** = patients with FECD with the trinucleotide repeat expansion; **RE−** = patients with FECD without the trinucleotide repeat expansion; **TCF4** = transcription factor 4 gene.

Keywords:
Confocal, Cornea, Fuchs' endothelial corneal dystrophy, Imaging, Scheimpflug.

Correspondence:
W. Matthew Petroll, PhD, 5323 Harry Hines Blvd, Dallas, TX 75390−9057. E-mail: Matthew.petroll@utsouthwestern.edu; and V. Vinod Mootha, MD, 5323 Harry Hines Blvd, Dallas, TX 75390−9057. E-mail: Vinod.mootha@utsouthwestern.edu.

References

1. Lorenzetti DW, Uotila MH, Parikh N, Kaufman HE. Central cornea guttata. Incidence in the general population. *Am J Ophthalmol*. 1967;64:1155−1158.
2. Gain P, Jullienne R, He Z, et al. global survey of corneal transplantation and eye banking. *JAMA Ophthalmol*. 2016;134:167−173.
3. Hogan MJ, Wood I, Fine M. Fuchs' endothelial dystrophy of the cornea. 29th Sanford Gifford Memorial lecture. *Am J Ophthalmol*. 1974;78:363−383.
4. Sarnicola C, Farooq AV, Colby K. Fuchs endothelial corneal dystrophy: update on pathogenesis and future directions. *Eye Contact Lens*. 2019;45:1−10.
5. Wieben ED, Aleff RA, Tosakulwong N, et al. A common trinucleotide repeat expansion within the transcription factor 4 (TCF4, E2-2) gene predicts Fuchs corneal dystrophy. *PLoS One*. 2012;7:e49083.
6. Mootha VV, Gong X, Ku HC, Xing C. Association and familial segregation of CTG18.1 trinucleotide repeat expansion of TCF4 gene in Fuchs' endothelial corneal dystrophy. *Invest Ophthalmol Vis Sci*. 2014;55:33−42.
7. Xing C, Gong X, Hussain I, et al. Transethnic replication of association of CTG18.1 repeat expansion of TCF4 gene with Fuchs' corneal dystrophy in Chinese implies common causal variant. *Invest Ophthalmol Vis Sci*. 2014;55:7073−7078.
8. Soliman AZ, Xing C, Radwan SH, et al. Correlation of severity of Fuchs endothelial corneal dystrophy with triplet repeat expansion in TCF4. *JAMA Ophthalmol*. 2015;133:1386−1391.
9. Mootha VV, Hussain I, Cunnusamy K, et al. TCF4 triplet repeat expansion and nuclear RNA foci in Fuchs' endothelial corneal dystrophy. *Invest Ophthalmol Vis Sci*. 2015;56:2003−2011.

10. Du J, Aleff RA, Soragni E, et al. RNA toxicity and missplicing in the common eye disease Fuchs endothelial corneal dystrophy. *J Biol Chem*. 2015;290:5979−5990.
11. Chu Y, Hu J, Liang H, et al. Analyzing pre-symptomatic tissue to gain insights into the molecular and mechanistic origins of late-onset degenerative trinucleotide repeat disease. *Nucleic Acids Res*. 2020;48:6740−6758.
12. Zhu AY, Jaskula-Ranga V, Jun AS. Gene editing as a potential therapeutic solution for Fuchs endothelial corneal dystrophy: the future is clearer. *JAMA Ophthalmol*. 2018;136:969−970.
13. Hu J, Rong Z, Gong X, et al. Oligonucleotides targeting TCF4 triplet repeat expansion inhibit RNA foci and mis-splicing in Fuchs' dystrophy. *Hum Mol Genet*. 2018;27:1015−1026.
14. Chau VQ, Hu J, Gong X, et al. Delivery of antisense oligonucleotides to the cornea. *Nucleic Acid Ther*. 2020;30:207−214.
15. Zarouchlioti C, Sanchez-Pintado B, Hafford Tear NJ, et al. Antisense therapy for a common corneal dystrophy ameliorates TCF4 repeat expansion-mediated toxicity. *Am J Hum Genet*. 2018;102:528−539.
16. Hu J, Shen X, Rigo F, et al. Duplex RNAs and ss-siRNAs Block RNA foci associated with Fuchs' endothelial corneal dystrophy. *Nucleic Acid Ther*. 2019;29:73−81.
17. Rong Z, Gong X, Hulleman JD, et al. Trinucleotide repeat-targeting dCas9 as a therapeutic strategy for Fuchs' endothelial corneal dystrophy. *Transl Vis Sci Technol*. 2020;9:47, 47.
18. Angelbello AJ, Benhamou RI, Rzuczek SG, et al. A small molecule that binds an RNA repeat expansion stimulates its decay via the exosome complex. *Cell Chem Biol*. 2021;28:34−45.e6.
19. Schrems-Hoesl LM, Schrems WA, Cruzat A, et al. Cellular and subbasal nerve alterations in early stage Fuchs' endothelial corneal dystrophy: an in vivo confocal microscopy study. *Eye (Lond)*. 2013;27:42−49.
20. Aggarwal S, Cavalcanti BM, Regali L, et al. In vivo confocal microscopy shows alterations in nerve density and dendritiform cell density in Fuchs' endothelial corneal dystrophy. *Am J Ophthalmol*. 2018;196:136−144.
21. Bucher F, Adler W, Lehmann HC, et al. Corneal nerve alterations in different stages of Fuchs' endothelial corneal dystrophy: an in vivo confocal microscopy study. *Graefes Arch Clin Exp Ophthalmol*. 2014;252:1119−1126.
22. Wacker K, McLaren JW, Amin SR, et al. Corneal high-order aberrations and backscatter in Fuchs' endothelial corneal dystrophy. *Ophthalmology*. 2015;122:1645−1652.
23. McLaren JW, Wacker K, Kane KM, Patel SV. Measuring corneal haze by using scheimpflug photography and confocal microscopy. *Invest Ophthalmol Vis Sci*. 2016;57:227−235.
24. Krachmer JH, Purcell Jr JJ, Young CW, Bucher KD. Corneal endothelial dystrophy. A study of 64 families. *Arch Ophthalmol*. 1978;96:2036−2039.
25. The definition and classification of dry eye disease: report of the Definition and Classification Subcommittee of the International Dry Eye WorkShop (2007). *Ocul Surf*. 2007;5:75−92.
26. Petroll WM, Cavanagh HD. Remote-controlled scanning and automated confocal microscopy through focusing using a modified HRT Rostock corneal module. *Eye Contact Lens*. 2009;35:302−308.
27. Petroll WM, Weaver M, Vaidya S, et al. Quantitative 3-dimensional corneal imaging in vivo using a modified HRT-RCM confocal microscope. *Cornea*. 2013;32:e36−e43.
28. Waldrop WH, Gillings MJ, Robertson DM, et al. Lower corneal haze and aberrations in descemet membrane endothelial keratoplasty versus descemet stripping automated endothelial keratoplasty in fellow eyes for Fuchs endothelial corneal dystrophy. *Cornea*. 2020;39:1227−1234.
29. Hirabayashi KE, Chamberlain W, Rose-Nussbaumer J, et al. Corneal light scatter after ultrathin descemet stripping automated endothelial keratoplasty versus descemet membrane endothelial keratoplasty in descemet endothelial thickness comparison trial: a randomized controlled trial. *Cornea*. 2020;39:691−696.
30. Li J, Jester JV, Cavanagh HD, et al. On-line 3-dimensional confocal imaging in vivo. *Invest Ophthalmol Vis Sci*. 2000;41:2945−2953.
31. Petroll WM, Robertson DM. In vivo confocal microscopy of the cornea: new developments in image acquisition, reconstruction, and analysis using the HRT-Rostock corneal module. *Ocul Surf*. 2015;13:187−203.
32. Vagenas D, Pritchard N, Edwards K, et al. Optimal image sample size for corneal nerve morphometry. *Optom Vis Sci*. 2012;89:812−817.
33. Afshari NA, Pittard AB, Siddiqui A, Klintworth GK. Clinical study of Fuchs corneal endothelial dystrophy leading to penetrating keratoplasty: a 30-year experience. *Arch Ophthalmol*. 2006;124:777−780.
34. Malik I, Kelley CP, Wang ET, Todd PK. Molecular mechanisms underlying nucleotide repeat expansion disorders. *Nat Rev Mol Cell Biol*. 2021;22:589−607.
35. Zhu AY, Eberhart CG, Jun AS. Fuchs endothelial corneal dystrophy: a neurodegenerative disorder? *JAMA Ophthalmol*. 2014;132:377−378.
36. Hunter A, Tsilfidis C, Mettler G, et al. The correlation of age of onset with CTG trinucleotide repeat amplification in myotonic dystrophy. *J Med Genet*. 1992;29:774−779.
37. Harley HG, Rundle SA, MacMillan JC, et al. Size of the unstable CTG repeat sequence in relation to phenotype and parental transmission in myotonic dystrophy. *Am J Hum Genet*. 1993;52:1164−1174.
38. Redman JB, Fenwick Jr RG, Fu YH, et al. Relationship between parental trinucleotide GCT repeat length and severity of myotonic dystrophy in offspring. *JAMA*. 1993;269:1960−1965.
39. Koh SWM, Waschek JA. Corneal endothelial cell survival in organ cultures under acute oxidative stress: effect of VIP. *Invest Ophthalmol Vis Sci*. 2000;41:4085−4092.
40. Koh SWM, Chandrasekara K, Abbondandolo CJ, et al. VIP and VIP gene silencing modulation of differentiation marker N-cadherin and cell shape of corneal endothelium in human corneas ex vivo. *Invest Ophthalmol Vis Sci*. 2008;49:3491−3498.
41. Sornelli F, Lambiase A, Mantelli F, Aloe L. NGF and NGF-receptor expression of cultured immortalized human corneal endothelial cells. *Mol Vis*. 2010;16:1439−1447.
42. Del Buey MA, Casas P, Caramello C, et al. An update on corneal biomechanics and architecture in diabetes. *J Ophthalmol*. 2019;2019:7645352.
43. Koh S, Maeda N, Ikeda C, et al. Ocular forward light scattering and corneal backward light scattering in patients with dry eye. *Invest Ophthalmol Vis Sci*. 2014;55:6601−6606.
44. Patel SV, McLaren JW. In vivo confocal microscopy of Fuchs endothelial dystrophy before and after endothelial keratoplasty. *JAMA Ophthalmol*. 2013;131:611−618.
45. Prasher P, Muftuoglu O, Bowman RW, et al. Tandem scanning confocal microscopy of cornea after descemet stripping automated endothelial keratoplasty. *Eye Contact Lens*. 2009;35:196−202.
46. Baratz KH, McLaren JW, Maguire LJ, Patel SV. Corneal haze determined by confocal microscopy 2 years after descemet

stripping with endothelial keratoplasty for Fuchs corneal dystrophy. *Arch Ophthalmol*. 2012;130:868–874.
47. Wacker K, Baratz KH, Maguire LJ, et al. Descemet stripping endothelial keratoplasty for Fuchs' endothelial corneal dystrophy: five-year results of a prospective study. *Ophthalmology*. 2016;123:154–160.
48. Wacker K, McLaren JW, Kane KM, et al. Corneal hydration control in Fuchs' endothelial corneal dystrophy. *Invest Ophthalmol Vis Sci*. 2016;57:5060–5065.
49. Wacker K, Grewing V, Fritz M, et al. Morphological and optical determinants of visual disability in Fuchs endothelial corneal dystrophy. *Cornea*. 2020;39:726–731.
50. Soh YQ, Peh Swee Lim G, Htoon HM, et al. Trinucleotide repeat expansion length as a predictor of the clinical progression of Fuchs' endothelial corneal dystrophy. *PLoS One*. 2019;14:e0210996.
51. McLaren JW, Bachman LA, Kane KM, Patel SV. Objective assessment of the corneal endothelium in Fuchs' endothelial dystrophy. *Invest Ophthalmol Vis Sci*. 2014;55:1184–1190.
52. Ong Tone S, Jurkunas U. Imaging the corneal endothelium in Fuchs corneal endothelial dystrophy. *Semin Ophthalmol*. 2019;34:340–346.
53. Patel SV. Imaging Fuchs endothelial corneal dystrophy in clinical practice and clinical trials. *Cornea*. 2021;40:1505–1511.